

Ensemble projection of 1–3°C warming in China

JIANG DaBang^{1,2,3†}, ZHANG Ying^{1,4} & SUN JianQi^{1,3}

¹Nansen-Zhu International Research Centre, Institute of Atmospheric Physics, Chinese Academy of Sciences, Beijing 100029, China;

²Max Planck Institute for Biogeochemistry, Jena D-07745, Germany;

³Climate Change Research Center, Chinese Academy of Sciences, Beijing 100029, China;

⁴Graduate University of Chinese Academy of Sciences, Beijing 100049, China

Studies on the influences of climate change on biogeochemical cycles and on the key vulnerabilities and the risk from climate change suggest that annual surface temperature rise of 1°C, 2°C and 3°C above the present level would lead to changes in extreme weather and climate events, food production, fresh water resources, biodiversity, human mortality, etc. Here two sets of simulations as performed with seventeen atmosphere-ocean general circulation models (AOGCMs) for the Fourth Assessment Report of the Intergovernmental Panel on Climate Change (IPCC AR4), i.e. the model outputs from the 20th Century Climate in Coupled Models (20C3M) and from the Special Report on Emissions Scenarios (SRES) emission scenarios B1, A1B and A2, are used to analyze spatial and temporal characteristics of the above values in China over the 21st century. The results indicate that the rate of warming varies from region to region. The above values are reached much later (earlier) when emission amount is lower (higher), and spread of the time when the lower (higher) value is exceeded is narrower (wider) among the three scenarios. As far as the spatial pattern is concerned, the above values are crossed much earlier in northern China and the Tibetan Plateau with respect to the Yangtze-Huaihe River Valley and South China.

surface temperature, warming, climate model, projection

Climate change is closely related to our living environment and has been one of the most important and active branches in geosciences. Global mean surface temperatures have risen by $0.74 \pm 0.18^\circ\text{C}$ over the 1906 to 2005 period and the rate of warming over the last 50 years is almost double that over the last 100 years^[1]. Under global warming, sustainable development of economy is greatly limited by climate change, environmental deterioration, ecological degeneration, etc. As well known, spatial and temporal climate conditions are quite complicated in China which is situated in the East Asian monsoon areas and adjacent to the western North Pacific. Furthermore, natural environmental conditions, highly influenced by geographic location and topographic and geomorphic features, are generally poor and most regions are susceptible and vulnerable to climate change.

While global warming is gradually intensified since the late 1970s, climate conditions in China undergo

some changes. For example, frequency of extreme weather and climate events, such as drought, flood, hot summer weather, and frost disasters, has increased, which impacts greatly social systems and causes considerable loss of national economy. Statistically, annual meteorological disasters can account for 3%–6% of the Gross Domestic Product of China during the 1990s, with a larger percentage in the years featured by significant climate anomalies^[2,3]. At the beginning of the 21st century, weather and climate disasters in China tend to intensify and lead to a much severer loss of industrial and agricultural production, national economy, and human life and property, which results in a variety of key social

Received February 2, 2009; accepted March 3, 2009; published online May 27, 2009
doi: 10.1007/s11434-009-0313-1

†Corresponding author (email: jiangdb@mail.iap.ac.cn)

Supported by the National Basic Research Program of China (Grant No. 2009CB421-407), National Key Technologies R&D Program Project (Grant No. 2007BAC03A01), Chinese Academy of Sciences (Grant No. KZCX2-YW-Q1-02) and National Natural Science Foundation of China (Grant No. 40775052)

and environmental problems. In the past few years, the extreme drought event in Chongqing in 2006, the heavy flood event in the Huaihe Valley in 2007, the disaster of low temperature, frozen rain, snow, and frost in South China in 2008, and the severe drought in northern China in 2009 are well known.

In the field of key vulnerabilities and the risk from climate change, some observed key impacts have been at least partly attributed to anthropogenic climate change. Among these include increases in human mortality, loss of glaciers, and rises in the frequency and/or intensity of extreme events such as heatwaves and tropical cyclones, all of which give rise to a series of severe social and environmental problems, especially in the areas vulnerable to climate change. Moreover, it is suggested that if annual surface temperature further exceeds several critical values of 1°C, 2°C, 3°C, 4°C and 5°C above the present level, the corresponding climate changes would impact heavily more social and environmental systems, e.g. food security and loss of biodiversity, particularly in developing countries where economic condition and public welfare are poor^[4]. Therefore, it is of importance to investigate spatial and temporal characteristics of the above critical values in China under global warming. In recent years, some works on climate change have been performed by Chinese scientists, such as numerical simulations of anthropogenic climate change using climate models^[5–18], analyses of climate change trend using available models' datasets^[19–26], and other pertinent projection researches^[27–29], etc. However, how the above critical values would evolve in China over the 21st century remains an open question so far.

Based on a variety of emission scenarios for atmospheric greenhouse gasses and aerosols, a number of climate models have been used to simulate anthropogenic climate change in the future, and globally averaged surface temperature is projected to increase by 1.1–6.4°C at 2090–2099 relative to 1980–1999^[30]. As such, assessing potential influences of climate change on socioeconomic systems and vulnerabilities and the risk from climate change in China is greatly important for understanding the future trend of climatic, environmental, and ecologic conditions and for making mitigation and adaptation strategies in the context of sustainable development of national economy. Therefore, datasets derived from seventeen AOGCMs participating in the IPCC AR4 are used to analyze spatial and temporal characteristics

of surface warming of 1°C, 2°C and 3°C in China over the 21st century in the present study.

1 Data and method

Twenty-three AOGCMs' simulations as forced by a series of emission scenarios are registered in the IPCC AR4. According to availability of integral surface temperature results derived from the SRES low (B1), medium (A1B), and high (A2) range emission scenarios^[31], seventeen IPCC AR4 AOGCMs' monthly surface temperature datasets for 2004 through 2099 are applied here. They are BCCR_BCM2.0, CCCMA_CGCM3.1 (T47), CNRM_CM3, CSIRO_Mk3.0, CSIRO_Mk3.5, GFDL_CM2.0, GFDL_CM2.1, GISS-ER, INMCM3.0, IPSL_CM4, MIROC3.2 (medres), ECHO_G, ECHAM5/MPI-OM, MRI_CGCM2.3.2, CCSM3.0, PCM1, and UKMO_HadCM3. More information about these state-of-the-art models can be found at the website http://www-pcmdi.llnl.gov/ipcc/about_ipcc.php. In addition, the above models' monthly surface temperature outputs from 1990 to 1999 in the 20C3M experiment are also utilized.

Every AOGCM is characterized by slightly or significantly different dynamical framework, physical and chemical processes, parameterization schemes, spatial and temporal resolutions, and so on. We therefore cannot expect the same responses even if these AOGCMs are forced by the same or similar emission scenarios for atmospheric greenhouse gasses and aerosols. Since the methodology to assess the fidelity of the AOGCMs' projections remains unresolved so far, each AOGCM projection is usually regarded as a probability of anthropogenic climate change in the future. At the same time, it is revealed that multi-model ensemble mean usually shows a higher reliability to reproduce the present East Asian climate relative to an individual model^[32–34]. Therefore, multi-model arithmetic mean with the same weights is applied here, which has been widely used in the projection of anthropogenic climate change^[30].

At present, levels of global mean temperature change are variously calculated in the literature with respect to the pre-industrial temperature in a specified year such as 1750 and 1850 or to the average temperature within a specified period such as the 1961–1990, 1980–1999, and 1990–2000 periods. Since the latter is mostly employed in the relevant chapters of the IPCC AR4^[4] and

the seventeen models' data are only partly available for 2000, the 1990–1999 period is chosen as the baseline period here. Given that horizontal resolution varies with model, the bilinear interpolation method is first applied to all of the AOGCMs' annual surface temperature data in order to generate uniform datasets with a consistent horizontal resolution of 5° by 5°. According to each of the SRES B1, A1B, and A2, three series of the seventeen-model ensemble mean surface temperature field from 2004 to 2099 are then figured out by use of the same weights. In the same way, baseline climatology of the seventeen-model ensemble mean surface temperature for the 1990 to 1999 period is calculated as well. Finally, three series of difference fields of the seventeen-model ensemble mean surface temperature for the 2004 to 2099 period, relative to the baseline climate, are obtained in terms of each scenario. It should be noted that influences of topographic differences among the models on interpolation results have been avoided when surface temperature differences between the above two periods are calculated.

Here, a preliminary evaluation of the models' fidelity to reproduce surface temperature climatology for the 1990 to 1999 period is performed with respect to the Climatic Research Unit (CRU) data with a horizontal resolution of 0.5° by 0.5°^[35]. In consideration of high horizontal resolution of the CRU surface temperature and topography data, an area-averaged extrapolation approach is used to obtain a coarse horizontal resolution of 5° by 5°. Since topography is found to vary with model when sixteen models' topographic data (the UKMO_HadCM3 topographic data are not available) are uniformly converted into a grid mesh of 5° by 5°, the effects of topographic difference on surface temperature

are taken into account when the seventeen-model ensemble mean surface temperature for the 1990 to 1999 period is calculated. Therein, an atmospheric lapse rate of 0.65°C per 100 m is assumed. Figure 1 shows that observational geographical distribution of annual surface temperature in East Asia is reasonably captured by the models on a large scale. For instance, in China, observational annual surface temperature is distributed zonally and drops northward, and a large extent of cooling appears over the Tibetan Plateau, which can be ascribed to *in situ* high topography. In general, the seventeen-model ensemble mean coincides well with the above spatial pattern. On the contrary, disagreements between the ensemble mean and observation are also presented, such as a cooling bias of annual surface temperature as simulated by the state-of-the-art models^[32–34], particularly over the Tibetan Plateau. In a quantitative way, spatial correlation coefficients between the CRU observation and each of the seventeen models and their ensemble mean are respectively figured out on the basis of forty-one grid points within China. The coefficients are 0.978 (BCCR_BCM2.0), 0.976 (CCCMA_CGCM3.1 (T47)), 0.968 (CNRM_CM3), 0.988 (CSIRO_Mk3.0), 0.992 (CSIRO_Mk3.5), 0.983 (GFDL_CM2.0), 0.987 (GFDL_CM2.1), 0.954 (GISS-ER), 0.969 (INMCM3.0), 0.991 (IPSL_CM4), 0.981 (MIROC3.2(medres)), 0.981 (ECHO_G), 0.988 (ECHAM5/MPI-OM), 0.961 (MRI_CGCM2.3.2), 0.987 (CCSM3.0), 0.988 (PCM1), 0.948 (UKMO_HadCM3), and 0.991 (ensemble mean). As such, the above models can dependably reproduce spatial pattern of annual surface temperature in China for the baseline period. As a whole, the ensemble mean shows a relatively high reliability, in line with the previous results^[32–34], which corroborates our approach to

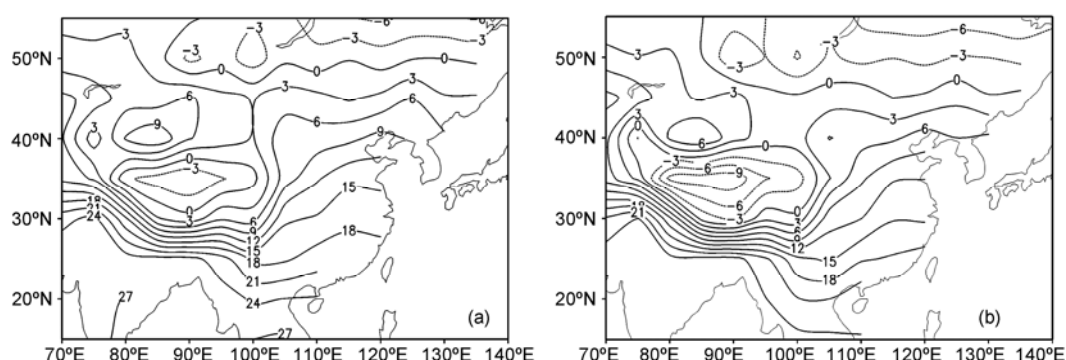


Figure 1 Mean annual surface temperature (Unit: °C) for the 1990 to 1999 period derived from the CRU observation data^[35] (a) and the seventeen-model ensemble mean in the 20C3M (b).

use multi-model ensemble mean.

2 Results

The territory of China consists of arid desert and Gobi regions in western parts, semiarid loess plateau and grassland regions in central parts, and semi-humid and humid regions in eastern parts. Large zonal and longitudinal width of the territory and topographic relief result in complexity of climate conditions. Towards a better understanding of how spatial and temporal characteristics of 1°C, 2°C and 3°C warmings above the baseline climate would evolve in the future, the above three series of difference fields of the seventeen-model ensemble mean surface temperature from 2004 to 2099 are respectively smoothed with a nine-year running mean. The reason behind is that the ensemble mean surface temperature, like that of an individual model, is also featured by inter-annual variability, and the running mean can exclude from signals of short-term climate variability, which is helpful to detecting relatively stable trend of surface temperature change.

2.1 Projection of 1–3°C warming for the whole China

Under global warming, it is interesting to take the mainland of China as a whole and then investigate how its annual surface temperature would evolve over time.

According to each scenario, three series of regionally averaged surface temperature changes over the 21st century, with respect to the baseline period, are respectively figured out on the basis of forty-one grid points within China. As shown in Figure 2, annual surface temperature would continue to rise in China. The rate of warming is slower in the SRES B1 than in the other two scenarios, and 1°C and 2°C warmings occur respectively in 2034 and 2072. The rate of warming is comparable between the SRES A1B and A2 before 2028. The rise of surface temperature is slightly large in the SRES A1B compared to A2 during 2028–2067, which agrees with synchronous changes of globally averaged surface temperature^[30] and can be attributed to more emission of greenhouse gasses in the early 21st century in the SRES A1B. Collectively, 1°C, 2°C and 3°C warmings are respectively registered in 2027 (2025), 2049 (2053) and 2074 (2071) in the SRES A1B (A2).

It is well known that models' behaviors are different when they are forced by same or similar forcings. In an attempt to estimate uncertainty of the above AOGCMs' results in China, standard deviation of annual surface temperature changes as derived from the seventeen AOGCMs is respectively calculated year by year in terms of each of the three scenarios. The shaded ranges embedded in Figure 2 indicate that there are disagreements among the projections of the seventeen AOGCMs.

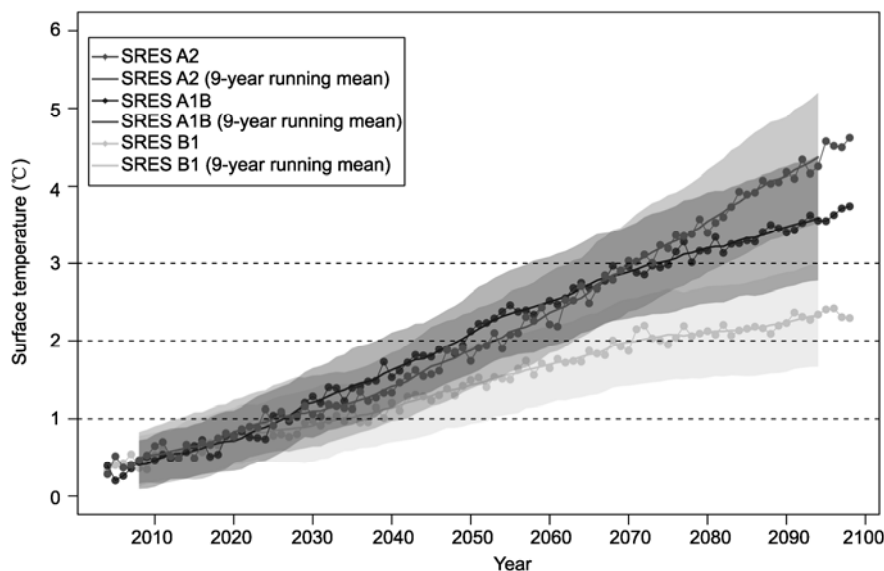


Figure 2 Seventeen-model ensemble mean annual surface temperature changes (relative to 1990–1999), regionally averaged within the mainland of China, for the SRES A2, A1B, and B1. For each scenario, shading denotes the ± 1 standard deviation range of individual model annual means after a nine-year running mean.

Moreover, like the case of synchronous global surface temperature projections^[30], the range of uncertainty becomes large over time on the whole.

2.2 Projection of 1°C warming

The geographical distribution of the year when 1°C, 2°C and 3°C warming of annual surface temperature is reached varies with region in each scenario. In general, the rate of warming is faster in northern China and the Tibetan Plateau, particularly for higher critical values. In the SRES B1, 1°C warming occurs firstly in western and central Tibet, western Qinghai and Gansu, Xinjiang, and most parts of Northeast China, and part of Inner Mongolia during 2025–2029, and then in the rest of Inner Mongolia, eastern and central Gansu and Qinghai, western Sichuan, and eastern Tibet in the early 2030s (Figure 3). After that, it is registered in North China, the lower reaches of Yellow and Huaihe Rivers, eastern Sichuan, and Chongqing during 2036–2039, and in the lower reaches of Yangtze River and South China in the early 2040s. The rate of 1°C warming is relatively slow in Taiwan (2049) and Hainan (2053).

With respect to the SRES B1, more emission of atmospheric greenhouse gasses is assumed in the SRES A1B, and the corresponding rate of warming is therefore faster. In China, 1°C warming is presented firstly in the areas west of 97.5°E, Northeast China, most parts of North China and Inner Mongolia, Qinghai, and western Gansu during 2021–2025, and then in western Sichuan, eastern Gansu, mid-western Inner Mongolia, and the lower reaches of Yellow and Huaihe Rivers in the late 2020s. Afterwards, it appears in the middle and lower reaches of Yangtze River and South China during 2030–2035. The rate of warming is still slow in Taiwan (2038) and Hainan (2041).

As far as the whole 21st century is concerned, total emission amount of atmospheric greenhouse gasses is larger in the SRES A2 than in the other two scenarios^[31], and the associated magnitude of global warming is therefore largest as a whole. However, total emission amount of atmospheric greenhouse gasses is comparable between the SRES A2 and A1B in the first half of the 21st century. Moreover, more emission amount is assumed in the latter scenario before 2020^[31]. As a result, the spatial pattern of the year when 1°C warming occurs in the SRES A2 agrees generally with that in the SRES

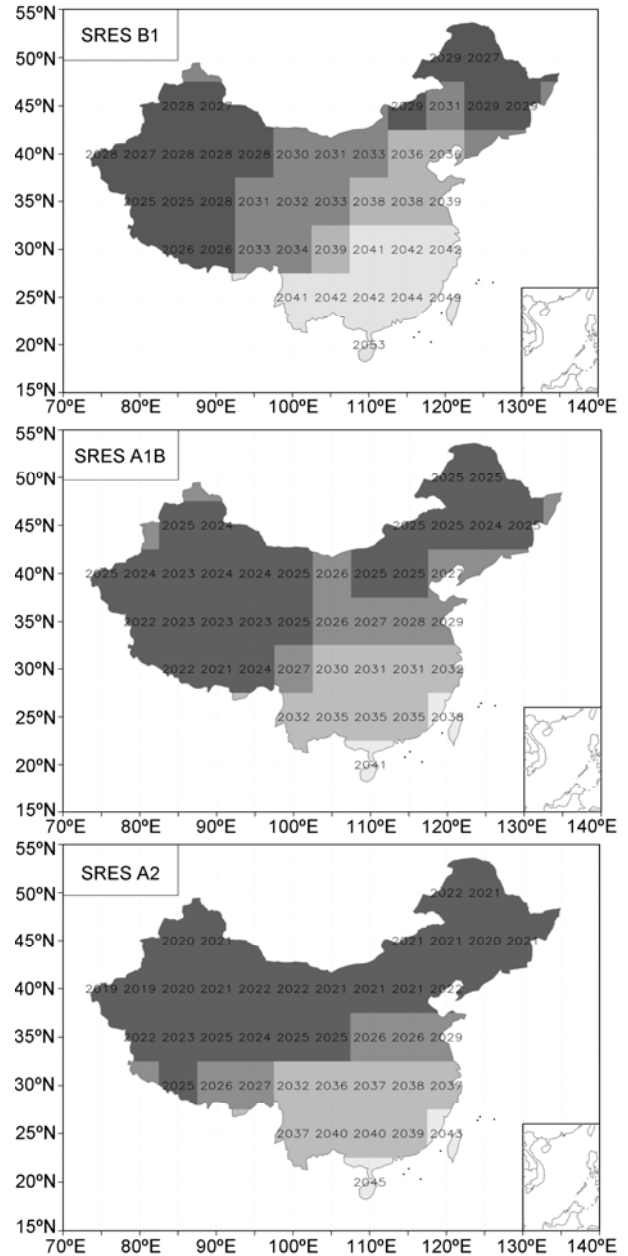


Figure 3 Geographical distribution of the time when 1°C warming of annual surface temperature above the baseline climate for 1990–1999, as projected by the seventeen-model ensemble mean where each model results are smoothed with a nine-year running mean, occurs in the SRES B1, A1B, and A2.

A1B, both of which are featured by a zonal distribution and a short time toward the north. Disagreement between each other lies in the fact that the rate of 1°C warming is 3–7 years slower (2–6 years faster) in the SRES A2 than in A1B in the areas south (north) of about 35°N.

It should be reminded that the above results are derived from the seventeen-model ensemble mean. Since

results vary from model to model, focusing on each of the forty-one grid points within China in each scenario, standard deviation of the time when 1°C warming appears is respectively calculated on the basis of the 17 AOGCMs' results in order to measure uncertainty of the ensemble mean. The results show that the standard deviation is largest in the SRES B1 and varies from 10 to 20 years with an average value of 14 years. In the SRES A2, it is on average 11 years with a range of 8 to 16 years. The standard deviation is smallest in the SRES A1B with an average value of 9 years and a range of 6 to 11 years. Therefore, it should be emphasized that there are disagreements among the seventeen AOGCMs' projections in China and the spread of uncertainty should be kept in mind when the seventeen-model ensemble mean described in the present study is referred to. By the way, standard deviation of the time when 2°C or 3°C warming appears is not analyzed hereinafter because these two values are not exceeded by part of the models in the 21st century in each of the three scenarios and uncertainty therefore cannot be measured by this statistical variable.

2.3 Projection of 2°C warming

At present, the time when 2°C warming of annual surface temperature above the 1990s would occur has been widely concerned. For example, the European Union has committed itself to limiting global warming to a maximum 2°C average temperature increase by reducing global emissions of greenhouse gases. It is suggested that if increase of annual surface temperature crosses this threshold, the corresponding climate changes would lead to a series of severe social, environmental, and ecological problems, such as increase in the risk of extreme weather and climate events (e.g., flood, drought, and heatwave)^[4]. It can be seen from Figure 4 that the rate of warming is slower in the SRES B1 than in the other two scenarios. 2°C warming occurs firstly in the areas north of 37.5°N, Qinghai, and Tibet during 2064–2069, and then respectively in eastern Gansu, Shaanxi, southern Shanxi, Henan, and southwestern Shandong in 2072, western Sichuan in 2078, and most parts of Shandong and Jiangsu in 2088. Finally, it occurs in eastern Sichuan, Chongqing, Hubei, northern Hunan and Jiangxi, southern Anhui, Zhejiang, and Shanghai during 2089–2093. In contrast, increase of surface temperature is less than 2°C in the rest of South China in the 21st century.

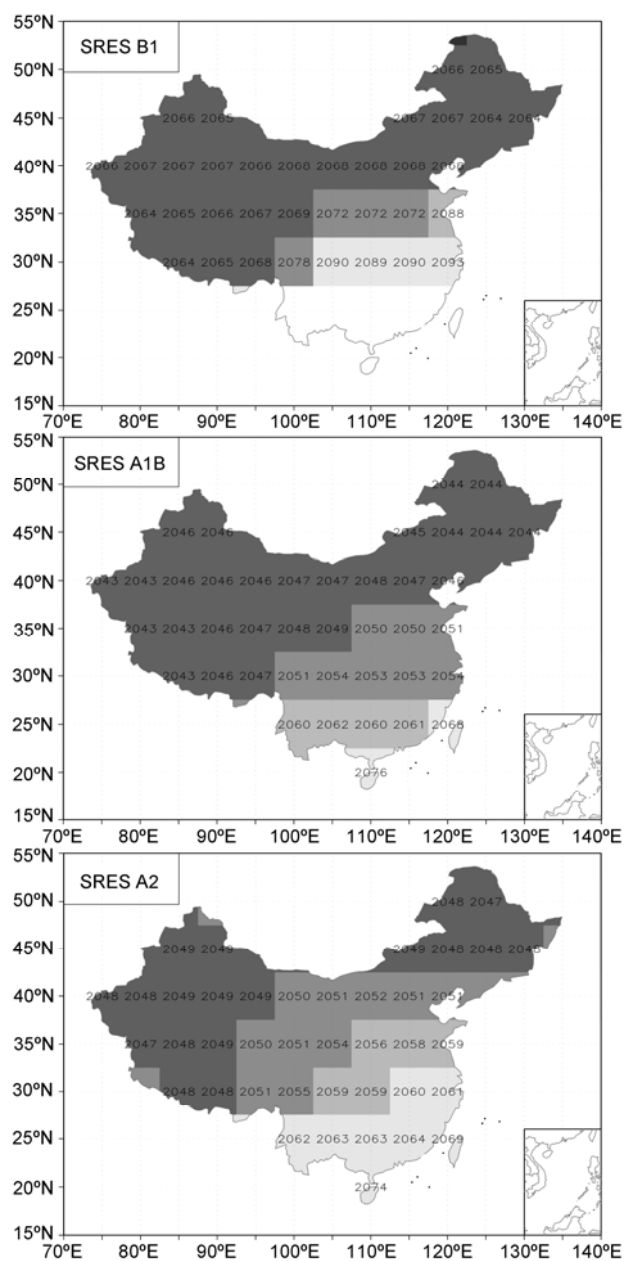


Figure 4 Same as in Figure 3, but for 2°C warming. Blanking denotes the magnitude of warming below 2°C in the 21st century.

The rate of warming is faster in the SRES A1B than in the above B1. 2°C warming is registered firstly in the areas north of 37.5°N, Gansu, Qinghai, and Tibet in around 2045, and then respectively in the lower reaches of Yangtze-Huaihe River Valley and the middle and lower reaches of Yangtze River in the early 2050s and in Yunnan, Guangdong, Guangxi, southern Hunan and Jiangxi, and southwestern Fujian during 2060–2061. The rate of warming is lowest in Taiwan (2068) and Hainan (2076).

In the SRES A2, 2°C warming occurs firstly in the

areas west of 92.5°E, western Gansu, and Northeast China during 2047–2049, and then in eastern Tibet, most parts of Qinghai and Gansu, central Inner Mongolia, and North China in the early 2050s. After that, it appears in the lower reaches of Yangtze River, Sichuan, Chongqing, southwestern Hubei, and northwestern Hunan in the late 2050s and in the rest of South China during 2060–2064. Finally, 2°C warming happens in Taiwan (2069) and Hainan (2074).

Intercomparison of the spatial pattern of the time when 2°C warming occurs between the SRES A1B and A2 (Figure 4) shows that the time is later in the SRES A2 than in A1B in the mainland of China excluding Hainan. The reason behind is that total emission amount of atmospheric greenhouse gasses is more in the SRES A1B than in A2 before 2020, although it remains comparable between these two scenarios in the first half of the 21st century^[31]. Since atmospheric lifetime of main greenhouse gasses is long (e.g., atmospheric lifetime of CO₂ is longer than one hundred years), more emission in the early period can generate a larger warming effect and consequently give rise to a faster rate of warming in the middle of the 21st century in the SRES A1B relative to A2.

2.4 Projection of 3°C warming

In the SRES B1, although annual surface temperature would continue to rise, the magnitude of warming is less than 3°C at the grid points within China by the end of the 21st century. Therefore, geographical distribution of the time for 3°C warming is only limited to the SRES A1B and A2 in Figure 5. In the SRES A1B, similar to the above spatial pattern of the time for 1°C or 2°C warming, 3°C warming occurs firstly in the areas west of 92.5°E, Northeast China, central and western Qinghai, and western Gansu and Inner Mongolia in the mid- and late 2060s and then in mid-western Inner Mongolia, northern Shaanxi and Shanxi, most parts of North China, eastern Qinghai and Gansu, and eastern Tibet in the early 2070s. After that, it occurs in western Sichuan, central Shaanxi, Henan, Shandong, and Jiangsu in the late 2070s and finally in the middle and lower reaches of Yangtze River and most parts of Yunnan in around 2090. In contrast, the magnitude of warming is less than 3°C in the rest of South China in the SRES A1B.

In the SRES A2, the rate of warming is fastest in the areas west of 97.5°E, Northeast China, eastern

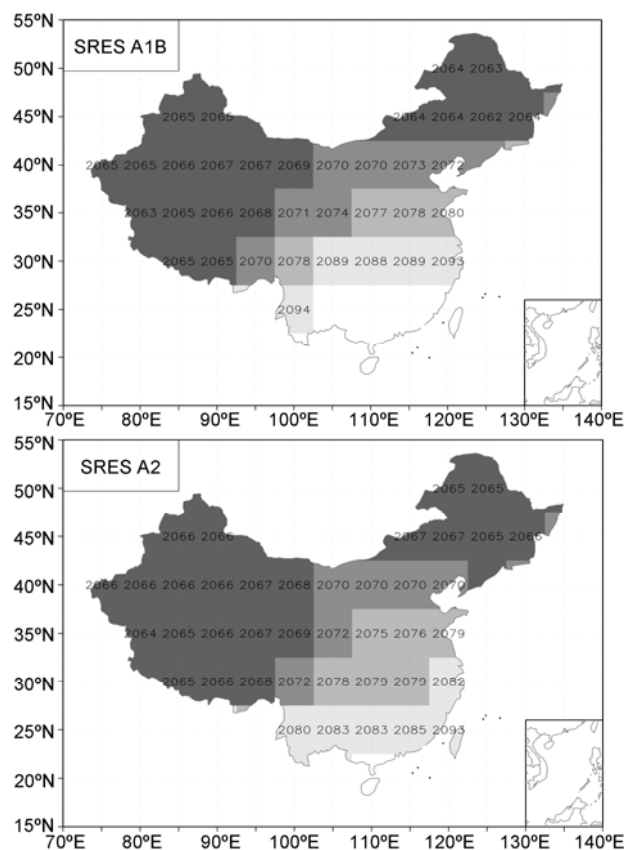


Figure 5 Same as in Figure 3, but for 3°C warming in the SRES A1B and A2. Blanking denotes the magnitude of warming below 3°C in the 21st century.

Qinghai, and western Gansu, where 3°C warming occurs during 2064–2069. Then, 3°C warming is registered in the lower reaches of Yellow River, eastern Gansu, and western Sichuan during 2070–2072, in the Yangtze-Huaihe River Valley and the middle reaches of Yangtze River in the mid-late 2070s, in the rest of South China during 2080–2085, and in Taiwan in 2093. In contrast, the magnitude of warming is less than 3°C in Hainan in the 21st century.

As mentioned above, total emission amount of atmospheric greenhouse gasses is comparable between the SRES A1B and A2 in the first half of the 21st century, and difference between each other mainly lies in the second half of the 21st century. As a result, the geographical distribution of the time when 3°C warming occurs is in general consistent between these two scenarios. It can be found that the time for 3°C warming is earlier in the mainland of China excluding Northeast China and northwestern Xinjiang in the SRES A2 than in A1B, implying that influence due to more emission of

atmospheric greenhouse gasses in the SRES A2, relative to the SRES A1B, emerges after the 2070s. Prior to this threshold time, surface temperature changes in China are comparable between the SRES A2 and A1B on the whole.

3 Conclusions

Based on the SRES emission scenarios B1, A1B, and A2 for atmospheric greenhouse gasses and aerosols, a number of climate models have been used to make projections of anthropogenic climate change over the 21st century. Here, two sets of simulations derived from the seventeen AOGCMs participating in the IPCC AR4 and 20C3M are used to analyze spatial and temporal characteristics of the time when 1°C, 2°C and 3°C warmings of annual surface temperature respectively occur in China by use of a multi-model ensemble projection. The primary conclusions are as follows:

(1) Taken the mainland of China as a whole, 1°C and 2°C warmings respectively occur in 2034 and 2072 in the SRES B1, and 1°C, 2°C and 3°C warmings are respectively registered in 2027 (2025), 2049 (2053) and 2074 (2071) in the SRES A1B (A2).

(2) The rate of warming varies with region in China. In summary, it is fastest in the areas west of about 97.5°E and Northeast China, and then in the reaches of Yellow and Yangtze Rivers. In contrast, the rate of warming is slowest in South China, Taiwan, and Hainan.

(3) In China, 1°C warming occurs respectively during 2025–2044 in the SRES B1, during 2021–2035 in the SRES A1B, and during 2019–2040 in the SRES A2. In addition, the rate of warming is slower in Taiwan and Hainan than in the rest of China.

(4) In the SRES B1, increase of annual surface temperature crosses 2°C during 2064–2093 in China excluding most parts of South China where the magnitude of warming is less than 2°C. The spatial pattern of the time for 2°C warming is well consistent between the SRES A1B and A2, and 2°C warming is consistently registered during 2043–2064. The rate of warming is still slowest in Taiwan and Hainan.

(5) Although annual surface temperature would continue to rise, the magnitude of warming is less than 3°C in China over the 21st century in the SRES B1. In the SRES A1B, 3°C warming occurs during 2062–2094 in China excluding most parts of South China where the magnitude of warming is below 3°C. 3°C warming is registered in the mainland of China during 2064–2085 and in Taiwan in 2093, whereas it is not exceeded in Hainan in the SRES A2.

Finally, we would like to stress that the above results should be regarded as state-of-the-art projections, by AOGCMs, of the spatial and temporal characteristics of the time when 1°C, 2°C and 3°C warmings of annual surface temperature respectively occur in China over the 21st century. In addition, uncertainties in the emission scenarios for atmospheric greenhouse gasses and aerosols and inadequacies in the formation of the AOGCMs give rise to the nature of uncertainty of the above AOGCMs' projections.

We thank anonymous reviewers for helpful comments. Also, we thank the modeling groups for making their model output available for analysis, the Program for Climate Model Diagnosis and Intercomparison (PCMDI) for collecting and archiving this data, and the WCRP's Working Group on Coupled Modelling (WGCM) for organizing the model data analysis activity. The WCRP CMIP3 multi-model dataset is supported by the Office of Science, U.S. Department of Energy.

- 1 Trenberth K E, Jones P D, Ambenje P, et al. Observations: Surface and Atmospheric Climate Change. In: Solomon S, Qin D, Manning M, et al., eds. *Climate Change 2007: The Physical Science Basis. Contribution of Working Group I to the Fourth Assessment Report of the Intergovernmental Panel on Climate Change*. Cambridge, United Kingdom and New York: Cambridge University Press, 2007. 236–336
- 2 Huang R H, Chen J L, Zhou L T, et al. Studies on the relationship between the severe climatic disasters in China and the East Asia climate system (in Chinese). *Chin J Atmos Sci*, 2003, 27: 770–787
- 3 Zhang R H. Research on theories and methods of monitoring and predicting of heavy rainfall in South China (in Chinese). *Chin Awards Sci Tech*, 2005. 74–77
- 4 Schneider S H, Semenov S, Patwardhan A, et al. Assessing key

vulnerabilities and the risk from climate change. In: Parry M L, Canziani O F, Palutikof J P, et al., eds. *Climate Change 2007: Impacts, Adaptation and Vulnerability. Contribution of Working Group II to the Fourth Assessment Report of the Intergovernmental Panel on Climate Change*. Cambridge, United Kingdom and New York: Cambridge University Press, 2007. 779–810

- 5 Wang H J, Zeng Q C, Zhang X H. The numerical simulation of the climatic change caused by CO₂ doubling. *Sci China Ser B*, 1993, 36: 451–462
- 6 Wang H J. The numerical simulation of the climate change of China induced by CO₂ doubling (in Chinese). *J Grad School Chin Acad Sci*, 1992, 9: 367–372
- 7 Chen Q Y, Yu Y Q, Guo Y F, et al. Climatic change in East Asia induced by greenhouse effect (in Chinese). *Clim Environ Res*, 1996, 1:

- 8 Chen K M, Zhang X H, Jin X Z, et al. A coupled ocean-atmosphere general circulation model for studies of global climate changes: II. Preliminary analyses on climate drift and enhanced greenhouse effect (in Chinese). *Acta Oceanol Sin*, 1997, 19: 26–40
- 9 Guo Y, Yu Y, Liu X, et al. Simulation of climate change induced by CO₂ increasing for East Asia with IAP/LASG GOALS model. *Adv Atmos Sci*, 2001, 18: 53–66
- 10 Gao X, Zhao Z, Ding Y, et al. Climate change due to greenhouse effects in China as simulated by a regional climate model. *Adv Atmos Sci*, 2001, 18: 1224–1230
- 11 Gao X, Zhao Z, Giorgi F. Changes of extreme events in regional climate simulations over East Asia. *Adv Atmos Sci*, 2002, 19: 927–942
- 12 Gao X J, Zhao Z C, Ding Y H, et al. Climate Change due to greenhouse effects in China as simulated by a regional climate model part II: climate change (in Chinese). *Acta Meteorol Sin*, 2003, 61: 29–38
- 13 Zhang Y J, Dong W J, Yu Y Q, et al. A prediction of trend of the future climate change in the western China (in Chinese). *Clim Environ Res*, 2004, 9: 342–349
- 14 Xu Y L, Zhang Y, Lin E, et al. Analyses on the climate change responses over China under SRES B2 scenario using PRECIS. *Chinese Sci Bull*, 2006, 51: 2260–2267
- 15 Zhang Y, Xu Y, Dong W, et al. A future climate scenario of regional changes in extreme climate events over China using the PRECIS climate model. *Geophys Res Lett*, 2006, 33: L24702, doi:10.1029/2006GL027229
- 16 Jiang Y, Wang S, Yang S, et al. Future trends of climatic belts and seasons in China. *Int J Climatol*, 2008, 28: 1483–1491
- 17 Shi Y, Gao X J. Influence of greenhouse effect on eastern China climate simulated by a high resolution regional climate model (in Chinese). *Chin J Atmos Sci*, 2008, 32: 1006–1018
- 18 Yu Y, Zhi H, Wang B, et al. Coupled model simulations of climate changes in the 20th century and beyond. *Adv Atmos Sci*, 2008, 25: 641–654
- 19 Bueh C. Simulation of the future change of East Asian monsoon climate using the IPCC SRES A2 and B2 scenarios. *Chinese Sci Bull*, 2003, 48: 1024–1030
- 20 Xu Y L, Xue F, Lin Y H. Changes of surface air temperature and precipitation in China during the 21st century simulated by HadCM2 under different greenhouse gas emission scenarios (in Chinese). *Clim Environ Res*, 2003, 8: 209–217
- 21 Xu Y, Ding Y H, Zhao Z C, et al. A scenario of seasonal climate change of the 21st century in Northwest China (in Chinese). *Clim Environ Res*, 2003, 8: 19–25
- 22 Zhao Z C, Ding Y H, Xu Y, et al. Detection and prediction of climate change for the 20th and 21st century due to human activity in Northwest China (in Chinese). *Clim Environ Res*, 2003, 8: 26–34
- 23 Jiang D B, Wang H J, Lang X M. Multimodel ensemble prediction for climate change trend of China under SRES A2 scenario. *Chin J Geophys*, 2004, 47: 878–886
- 24 Ding Y, Ren G, Zhao Z, et al. Detection, causes and projection of climate change over China: an overview of recent progress. *Adv Atmos Sci*, 2007, 24: 954–971
- 25 Zhang Y, Xu Y L, Dong W J, et al. A preliminary analysis of distribution characteristics of maximum and minimum temperature and diurnal temperature range changes over China under SRES B2 scenario. *Chin J Geophys*, 2007, 50: 632–642
- 26 Zhu Y L, Wang H J. The Arctic and Antarctic oscillations in the IPCC AR4 coupled models (in Chinese). *Acta Meteorol Sin*, 2008, 6: 993–1004
- 27 Wu S H, Dai E F, Huang M, et al. Ecosystem vulnerability of China under B2 climate scenario in the 21st century. *Chinese Sci Bull*, 2007, 52: 1379–1386
- 28 Yao F M, Zhang J H, Sun B N, et al. Simulation and analysis of effects of climate change on rice yields in southern China (in Chinese). *Clim Environ Res*, 2007, 12: 659–666
- 29 Jiang D. Projected potential vegetation change in China under the SRES A2 and B2 scenarios. *Adv Atmos Sci*, 2008, 25: 126–138
- 30 Meehl G A, Stocker T F, Collins W D, et al. Global Climate Projections. In: Solomon S, Qin D, Manning M, et al., eds. *Climate Change 2007: The Physical Science Basis. Contribution of Working Group I to the Fourth Assessment Report of the Intergovernmental Panel on Climate Change*. Cambridge and New York: Cambridge University Press, 2007. 748–845
- 31 Nakićenović N, Alcamo J, Davis G, et al. *IPCC Special Report on Emissions Scenarios*. Cambridge: Cambridge University Press, 2000. 1–599
- 32 Jiang D, Wang H J, Lang X. Evaluation of East Asian climatology as simulated by seven coupled models. *Adv Atmos Sci*, 2005, 22: 479–495
- 33 Zhou T, Yu R. Twentieth-century surface air temperature over China and the global simulated by coupled climate models. *J Clim*, 2006, 19: 5843–5858
- 34 Xu C H, Shen X Y, Xu Y. An analysis of climate change in East Asia by using the IPCC AR4 simulations (in Chinese). *Adv Clim Change Res*, 2007, 3: 287–291
- 35 Mitchell T D, Jones P D. An improved method of constructing a database of monthly climate observations and associated high-resolution grids. *Int J Climatol*, 2005, 25: 693–712